ARTICLE IN PRESS
Ain Shams Engineering Journal (2015) xxx, xxx–xxx

Ain Shams University
Ain Shams Engineering Journal
www.elsevier.com/locate/asej
www.sciencedirect.com

ENGINEERING PHYSICS AND MATHEMATICS

Radiative nanofluid flow and heat transfer over a non-linear permeable sheet with slip conditions and variable magnetic field: Dual solutions

Puneet Rana *, Ruchika Dhanai, Lokendra Kumar

Department of Mathematics, Jaypee Institute of Information Technology, Noida, U.P., India

Received 2 April 2015; revised 27 July 2015; accepted 2 August 2015

KEYWORDS

MHD;
Nanofluids;
Stretching sheet;
Dual solution;
Thermal radiation;
Viscous dissipation

Abstract *Objective:* This paper addresses numerical investigation of steady, magneto-hydrodynamic boundary-layer slip flow of a nanofluid past a permeable stretching/shrinking sheet with thermal radiation using RKF45 with shooting technique. The effect of viscous dissipation, suction/injection, Brownian motion, thermophoresis, partial velocity slip and thermal slip is taken into account and controlled by the non-dimensional parameters.

Results and conclusions: The dual solutions are obtained for the skin friction, Nusselt number, temperature and nanoparticle volume fraction with pertinent parameters in the domain (χ_c, ∞) and (s_c, ∞). The study shows that the Nusselt number decreases with an increase in thermophoresis parameter Nt and thermal slip parameter δ but increases with thermal radiation R and Prandtl number Pr.

Practice implications: The present problem has numerous applications in engineering and petroleum industries such as glass blowing, annealing and thinning of copper wires. The study of radiation heat transfer plays an important role in the industrial applications at high temperature.

1. Introduction

The vast study has been carried out by several researchers in the field of boundary layer flow and convective heat transfer over a stretching/shrinking sheet due to various applications in the industries and engineering process such as glass blowing, annealing and thinning of copper wires. It is obvious that the desired quality of final sheet strongly depends on the stretching rate and the rate of cooling (heat transfer) in the process of stretching. First analysis on the boundary layer flow over a stretching sheet was studied by Crane [1]. This study is extended by many researchers to examine the various aspects of flow and heat transfer characteristics. Khan and Pop [2] studied the behavior of Nusselt number and Sherwood number for the boundary layer flow of a nanofluid over a linearly stretching sheet under the consideration of two-component model. Instead of linear stretching of sheet, the quality of sheet can also be controlled with nonlinear and exponentially

* Corresponding author. Mobile: +91 9711333514.
E-mail address: puneetranaiitr@gmail.com (P. Rana).
Peer review under responsibility of Ain Shams University.

ELSEVIER Production and hosting by Elsevier

http://dx.doi.org/10.1016/j.asej.2015.08.016
2090-4479 © 2015 Faculty of Engineering, Ain Shams University. Production and hosting by Elsevier B.V.

Please cite this article in press as: Rana P et al., Radiative nanofluid flow and heat transfer over a non-linear permeable sheet with slip conditions and variable magnetic field: Dual solutions, Ain Shams Eng J (2015), http://dx.doi.org/10.1016/j.asej.2015.08.016

Nomenclature

a	constant
B_0	magnetic field strength (A/m)
C	nanoparticle volume fraction
C_∞	ambient volume fraction
$B(x)$	variable magnetic field (A m^{m-2})
D_B	Brownian diffusion coefficient (m^2/s)
D_T	thermophoretic diffusion coefficient (m^2/s)
Ec	Eckert number
f	dimensionless stream function
k	thermal conductivity (W/m K)
Sc	Schmidt number
L	velocity slip factor (m)
m	power index
M	dimensionless magnetic field
N	thermal slip factor (m)
Nb	Brownian motion parameter
Nt	thermophoresis parameter
Pr	Prandtl number
R	dimensionless thermal radiation
s	mass transfer parameter
T	nanofluid temperature (K)
T_w	nanofluid temperature at sheet (K)
T_∞	ambient temperature (K)
u, v	velocity components along x- and y-axis (m/s)
u_w	velocity of sheet (m/s)
v_w	mass transfer velocity (m/s)
x, y	Cartesian coordinates (m)
q_r	radiative heat flux (W/m^2)

Greek symbol

η	similarity variable
μ	dynamic viscosity (Ns/m^2)
ν	kinematic viscosity (m^2/s)
ϕ	rescaled nanoparticle volume fraction
θ	dimensionless temperature
χ	stretching/shrinking parameter
σ	electric conductivity of base fluid (S/m)
$(\rho c)_f$	heat capacity of base fluid (J/K)
$(\rho c)_p$	effective heat capacity of nanoparticle material (J/K)
σ^*	Stefan–Boltzmann constant (W m^{-2} K^{-4})
β	power-law parameter
τ_w	shear stress at surface (N/m^2)
δ	thermal slip parameter

Subscript

∞	ambient condition
w	condition on surface
r	radiation
f	base fluid
s	slip condition

stretching along with consideration of heat and mass transfer characteristics. Motivated by this concept, Cortell [3] has discussed viscous flow and heat transfer over a nonlinearly stretching sheet. Rana and Bhargava [4] have extended the idea to nanofluids and employed finite element method for the numerical computation of flow and heat transfer characteristic over a nonlinearly stretching sheet. Moreover, analytical solution of the boundary layer flow over an exponential stretching sheet has been investigated (Nadeem and Lee [5]) using homotopy analysis method.

Since last few years many researchers are attracted towards nanofluid due to its enhanced thermal conductivity as compared to base fluids that are responsible for heat transfer. Nanofluid, which was first introduced by Choi [6], is dilute suspension of nanometer sized solid particle (Cu, Al, Ag, etc.) in base fluid such as water, oil and ethylene glycol. The novel characteristics of nanofluids can be utilized to develop stable suspensions with improved heat transfer. Many researchers have tried to develop the convective transport models for nanofluid. In 2006, Buongiorno [7] has presented non-homogeneous model to understand the convective transport phenomena in nanofluid and studied seven-slip mechanisms. Among these mechanisms only Brownian diffusion and thermophoresis diffusion are found most important. These two slip mechanisms are also incorporated in the study of natural convective boundary layer flow of a nanofluid over a vertical plate by Kuznetsov and Nield [8].

The study of magnetohydrodynamic has numerous applications in engineering, agriculture and petroleum industries. The problem of natural convection under the effect of a magnetic field has also applications in geophysics and astrophysics [9]. Due to this many studies were performed with the effect of magnetic field. Fang and Zhang [10] have given exact solution for MHD flow equation of fluid over a shrinking sheet. They have reported two solution branches for $M \in (0,1)$ but for $M = 1$ single solution branch is obtained only in case of suction and when $M > 1$ there is also single branch of solution for both suction and injection. In 2011, Hamad [11] investigated the analytical solution of electrical conducting nanofluid flow over a linearly stretching sheet under the influence of magnetic field. He found that momentum boundary layer thickness decreases but thermal boundary thickness increases with magnetic field. Rana et al. [12] presented unsteady MHD transport phenomena over a stretching sheet in a rotating nanofluid. Numerical investigation of the MHD flow and heat transfer of nanofluid between two horizontal plates in rotating system using Cu, Ag, Al_2O_3 and TiO_2 nanoparticles in water has been computed by Sheikholeslami et al. [13] and it is noticed that heat transfer is the highest for TiO_2 nanoparticles. Currently, much attention has been devoted to work in the presence of magnetic field [14–18].

Several engineering processes occur due to high temperature; therefore, the study of radiation heat transfer plays an important role in the field of equipment designing [19]. Cortell [20] analyzed the boundary layer flow and heat transfer of fluid under the consideration of thermal radiation and viscous dissipation over a nonlinear stretched sheet. This work is extended by Hady et al. [21] in nanofluid and investigated the effect of thermal radiation, viscous dissipation and nanoparticle volume fraction on velocity, temperature and the rate of heat transfer at the surface. They noticed that an increase in thermal radiation decreases temperature of nanofluid which leads

Please cite this article in press as: Rana P et al., Radiative nanofluid flow and heat transfer over a non-linear permeable sheet with slip conditions and variable magnetic field: Dual solutions, Ain Shams Eng J (2015), http://dx.doi.org/10.1016/j.asej.2015.08.016

to increment in rate of heat transfer whereas temperature increases with viscous dissipation which gives sudden fall in rate of heat transfer. Motsumi and Makinde [22] have studied the boundary layer flow over a permeable moving flat plate under the effect of viscous dissipation and thermal radiation by considering Cu-water and Al_2O_3-water nanofluids Furthermore, Pal et al. [23] have studied the heat transfer over non-linear stretching and shrinking sheets under the influence of magnetic field, thermal radiation and viscous dissipation by considering copper (Cu), alumina (Al_2O_3), and titanium oxide (TiO_2) nanoparticles. Recently, Nandy and Pop [24] extended the work of Khan and Pop [2] by examining the study of MHD boundary layer stagnation flow and heat transfer over a shrinking sheet incorporating the two component model under the effect of radiation. Very recently, Sheikholeslami et al. [25] studied the combined effect of magnetic field and thermal radiation for nanofluid flow and heat transfer between two horizontal parallel plates by considering two-component model. Rashidi et al. [26] have also investigated the combined effect of magnetic field and thermal radiation over a vertical stretching sheet for two dimensional water based nanofluid flow. They observed that velocity decreases and temperature increases in the presence of magnetic field and skin friction increases with magnetic field and thermal radiation.

Most of the studies are carried out without slip condition, i.e. it is assumed that fluid particles have zero velocity relative to solid boundary. But literature shows that the characteristics are different in case of micro- and nano-scale fluid flow. Thus, the importance of slip boundary condition was first discussed by Navier [27], which states that fluid slip is proportional to shear stress. In 2002, Wang [28] has given the exact solution of Navier–Stokes equations for the flow over a stretching sheet by taking into account partial slip. Fang et al. [29] also investigated the analytical solution for slip effect over a shrinking sheet considering magnetic field effect and noticed the multiple, single and no solution exist for $0 < M < 1$, $M = 1$, and $M > 1$, respectively. Recently, Das [30,31] investigated the partial slip flow and convective heat transfer of nanofluids over a linear and nonlinear stretching sheet. Moreover, Ibrahim and Shankar [32] incorporated the effect of velocity, thermal and solutal slip boundary condition over a stretching sheet to study the MHD boundary layer flow and heat transfer of a nanofluid. Currently, Uddin et al. [33] have studied hydromagnetic boundary layer slip flow of bio-nanofluid which is significant to the synthesis of bio-magnetic nanofluids of potential interest in skin repair, wound treatments and coatings for biological devices. Multiple solutions for fluid flow and heat transfer are also a point of attraction of various researchers. The survey of recent literatures shows the existence of more than one solution for boundary layer flow over stretching/shrinking sheet [34–38].

The main concern of current study is to investigate the dual solution for the combined effects of thermal radiation, magnetic field, mass suction transfer, and viscous dissipation for steady boundary layer nanofluid flow over a power- law stretching/shrinking sheet in the presence of partial slip by using Nield and Kuznetsov revised nanofluid model [8]. As authors knowledge no efforts are devoted for this kind of problem. Motivated by this fact, present study analyzes the variation of skin friction, Nusselt number, temperature and nanoparticle concentration in the presence of abovementioned parameters numerically by using shooting method [39] with RKF45 method and presented graphically in this paper.

2. Nanofluid transport model

We consider a steady, laminar, two dimensional boundary layer flow of incompressible and electrically conducting nanofluid along a horizontal nonlinear stretching/shrinking sheet under the effect of viscous dissipation and thermal radiation. The coordinate system is considered as, x-axis is taken along the sheet and y-axis perpendicular to the sheet (see Fig. 1). The fluid is moving due to nonlinear stretching/shrinking of the sheet caused by two parallel forces act in opposite direction along the x-axis. The sheet is stretched/shrunk with velocity $u_w(x) = ax^m$, where a is a constant, m is a power index and wall mass suction/injection velocity is $v_w = v_w(x)$, by keeping the origin 'O' fixed. The variable magnetic field $B(x)$ is assumed to be applied along y-axis. The radiative heat flux q_r is also taken perpendicular (y-axis) to the sheet. The temperature at sheet T_w is assumed to be constant and the ambient temperature is T_∞, as $y \to \infty$ where $T_\infty < T_w$. The nanoparticle volume fraction is assumed to be controlled passively on the sheet by the temperature gradient. The ambient nanoparticle volume fraction is C_∞. The external forces and pressure gradient are assumed to be zero. Under these hypotheses, the steady conservation equations for proposed nanofluid model are presented in Cartesian coordinates x, y as (see [7,8,21,31,40])

$$\frac{\partial u}{\partial x} + \frac{\partial v}{\partial y} = 0 \tag{1}$$

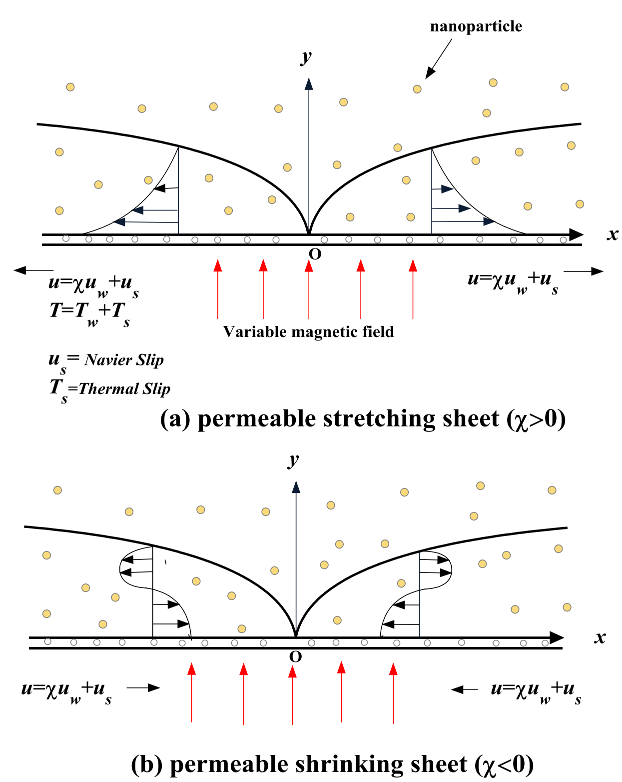

Figure 1 Physical model and the coordinate system.

Please cite this article in press as: Rana P et al., Radiative nanofluid flow and heat transfer over a non-linear permeable sheet with slip conditions and variable magnetic field: Dual solutions, Ain Shams Eng J (2015), http://dx.doi.org/10.1016/j.asej.2015.08.016

$$u\frac{\partial u}{\partial x}+v\frac{\partial u}{\partial y}=v\frac{\partial^2 u}{\partial y^2}-\frac{\sigma B^2}{\rho}u \tag{2}$$

$$(\rho c)_f\left(u\frac{\partial T}{\partial x}+v\frac{\partial T}{\partial y}\right)=k\frac{\partial^2 T}{\partial y^2}-\frac{\partial q_r}{\partial y}+(\rho c)_p\left(D_B\left(\frac{\partial C}{\partial y}\right)\left(\frac{\partial T}{\partial y}\right)+\frac{D_T}{T_\infty}\left(\frac{\partial T}{\partial y}\right)^2\right)+\mu\left[\frac{\partial u}{\partial y}\right]^2 \tag{3}$$

$$u\frac{\partial C}{\partial x}+v\frac{\partial C}{\partial y}=D_B\frac{\partial^2 C}{\partial y^2}+\frac{D_T}{T_\infty}\frac{\partial^2 T}{\partial y^2} \tag{4}$$

In Eq. (2), we have ignored the induced magnetic field because of small magnetic Reynolds number for fluid motion. The external electric field and electric field due to polarization of charges are also neglected and the magnetic field is of the form [41]:

$$B(x)=B_0x^{(m-1)/2} \tag{5}$$

where m is power index.

Here u and v are the velocity components along the x- and y-axis, respectively, ρ_f and ρ_p are the base fluid and nanoparticle densities respectively. μ is the dynamic viscosity, v is the kinematic viscosity, σ is the electrical conductivity of the base fluid, T is the temperature, c_f and c_p are the specific heat of base fluid and nanoparticle at fixed pressure, respectively and k is the thermal conductivity. C is concentration of nanoparticles, D_B is Brownian motion and D_T is thermophoretic diffusion coefficient. The boundary conditions are as follows (see [8,32,38]):

$$u=\chi u_w(x)+u_s,\quad v=v_w(x),\quad T=T_w+T_s,\quad D_B\frac{\partial C}{\partial y}+\frac{D_T}{T_\infty}\frac{\partial T}{\partial y}=0\quad \text{at } y=0 \tag{6a}$$

$$u=0,\quad v=0,\quad T=T_\infty,\quad C=C_\infty\quad \text{as } y\to\infty \tag{6b}$$

where χ is stretching (for positive)/shrinking (for negative) parameter, u_s is slip velocity which is assumed equal to $L\frac{\partial u}{\partial y}$ and T_s is thermal slip equal to $N\frac{\partial T}{\partial y}$.

q_r is considered insignificant in x-direction and defined by applying Rosseland approximation for optically thick media, as (see [21,42,43]):

$$q_r=\frac{-4}{3k^*}grad(e_b) \tag{7}$$

where k^* is the Rosseland mean spectral absorption coefficient and e_b is the blackbody emission power, defined by the Stefan–Boltzmann radiation law $e_b=\sigma^*T^4$. Hence

$$q_r=\frac{-4\sigma^*}{3k^*}\frac{\partial T^4}{\partial y}. \tag{8}$$

The temperature difference inside the flow is assumed to be very small so T^4 can be expressed as a linear function of temperature, by applying Taylor series expansion about T_∞ such that

$$T^4=T_\infty^4+4T_\infty^3(T-T_\infty)+6T_\infty^2(T-T_\infty)^2+\dots \tag{9}$$

higher order terms of $(T-T_\infty)$ in above Eq. (9) are neglected, then we get

$$T^4\approx 4T_\infty^3T-3T_\infty^4. \tag{10}$$

Using Eq. (10) in Eq. (8), we obtain

$$q_r=-\frac{4\sigma^*}{3k^*}\frac{\partial}{\partial y}\left(4T_\infty^3T-3T_\infty^4\right)=-\frac{16\sigma^*T_\infty^3}{3k^*}\frac{\partial T}{\partial y}. \tag{11}$$

and

$$\frac{\partial q_r}{\partial y}=-\frac{16\sigma^*T_\infty^3}{3k^*}\frac{\partial^2 T}{\partial y^2}. \tag{12}$$

Now we introduce the following similarity variables for Eqs. (1)–(4) with boundary conditions (6):

$$\psi=\sqrt{\frac{2va}{m+1}}x^{\frac{m+1}{2}}f(\eta),\quad \eta=y\sqrt{\frac{a(m+1)}{2v}}x^{\frac{m-1}{2}},$$
$$\theta(\eta)=\frac{T-T_\infty}{T_w-T_\infty},\quad \phi(\eta)=\frac{C-C_\infty}{C_\infty},$$

where ψ is the stream function, which is defined as $u=\frac{\partial\psi}{\partial y}$ and $v=-\frac{\partial\psi}{\partial x}$. Thus, we have

$$u=ax^mf'(\eta),\quad v=-\sqrt{\frac{av(m+1)}{2}}x^{\frac{m-1}{2}}\left[f(\eta)+\frac{m-1}{m+1}\eta f'(\eta)\right]. \tag{13}$$

Hence using similarity variables the governing Eqs. (2)–(4) transform to

$$f'''+ff''-\beta f'^2-M^2f'=0 \tag{14}$$

$$\left(1+\frac{4R}{3}\right)\theta''+Nb\theta'\phi'+Nt\theta'^2+Pr\left(f\theta'+Ecf''^2\right)=0 \tag{15}$$

$$\phi''+Scf\phi'+\frac{Nt}{Nb}\theta''=0 \tag{16}$$

and boundary conditions become

$$\text{at } \eta=0,\quad f=s,\quad f'=\chi+\lambda f'',\quad \theta=1+\delta\theta',\quad Nb\phi'+Nt\theta'=0,$$
$$\text{as } \eta\to\infty,\quad f'=0,\quad \theta=0,\quad \phi=0, \tag{17}$$

where prime denotes the differentiation with respect to η only and $\beta=\frac{2m}{m+1}$ power-law parameter, $M=\sqrt{\frac{2\sigma B_0^2}{a\rho_f(m+1)}}$ is Hartman number or magnetic field parameter, $Pr=\frac{(\rho c)_f v}{k}$ is Prandtl number, $Sc=\frac{v}{D_B}$ is Schmidt number, $Ec=\frac{u_w^2}{c_f(T_w-T_\infty)}$ is Eckert number, $R=\frac{4\sigma^*T_\infty^3}{k^*k}$ is radiation parameter, $Nb=\frac{(\rho c)_pD_BC_\infty}{(\rho c)_f\alpha}$ is Brownian motion parameter, $Nt=\frac{(\rho c)_pD_T(T_w-T_\infty)}{(\rho c)_f\alpha T_\infty}$ is thermophoresis parameter, $s=-\frac{v_w}{\sqrt{\frac{av(m+1)}{2}}x^{\frac{m-1}{2}}}$ is mass transfer parameter, i.e. suction for $(v_w<0)$ and injection for $(v_w>0)$, $\lambda=L\sqrt{\frac{a(m+1)}{2v}}x^{\frac{m-1}{2}}$ is the velocity slip parameter, and $\delta=N\sqrt{\frac{a(m+1)}{2v}}x^{\frac{m-1}{2}}$ is the thermal slip parameter.

The important physical quantities in this study are the skin friction coefficient and the local Nusselt number which are defined as

$$C_f=\frac{\tau_w}{\rho u_w^2},\quad Nu_x=\frac{xq_w}{k(T_w-T_\infty)}, \tag{18}$$

where τ_w is shear stress at wall and q_w is the wall heat flux which are given below:

$$\tau_w = \mu\left(\frac{\partial u}{\partial y}\right)_{y=0}, \quad q_w = -\left(k + \frac{16\sigma^* T_\infty^3}{3k^*}\right)\left(\frac{\partial T}{\partial y}\right)_{y=0}. \tag{19}$$

Using Eqs. (13) and (19) in Eq. (18), we get

$$C_f Re^{1/2} = f''(0) \quad \text{and} \quad \frac{Nu_x}{Re^{1/2}} = -\left(1 + \frac{4}{3}R\right)\theta'(0),$$

where $Re = \frac{a(m+1)}{2\upsilon}x^{m+1}$ is Local Reynolds number and Reduced Nusselt number is given by

$$Nur = -\left(1 + \frac{4}{3}R\right)\theta'(0). \tag{20}$$

A closed analytical solution for MHD slip flow $f''' + ff'' - f'^2 - M^2 f' = 0$ over a shrinking sheet has been obtained by Fang et al. [29], which is given as

$$f(\eta) = s - \frac{1}{\zeta + \lambda\zeta^2} + \frac{1}{\zeta + \lambda\zeta^2}e^{-\zeta\eta}, \tag{21}$$

and

$$f'(\eta) = -\frac{1}{1 + \lambda\zeta}e^{-\zeta\eta}, \quad f''(0) = \frac{\zeta}{1 + \lambda\zeta}, \tag{22}$$

where s is mass transfer parameter, λ is velocity slip parameter and ζ is root of the Eq. $\lambda\zeta^3 + (1 - s\lambda)\zeta^2 - (s + \lambda M^2)\zeta + 1 - M^2 = 0$. Only positive real roots of ζ are physically feasible solutions. There may be either three real roots or one real and two complex conjugate roots or one simple real and two two-fold real roots or one threefold real roots depending on the values of M, s and λ. For $M < 1$ multiple solutions are observed for all values of λ and the domain of multiple solutions is changed with λ. For $M = 1$, only one solution branch exists and when $M > 1$, there is one solution for both mass suction and injection [29].

3. Stability analysis

The stability of the solutions is investigated by considering unsteady flow of present nanofluid model which is given as

$$\frac{\partial u}{\partial x} + \frac{\partial v}{\partial y} = 0, \tag{23}$$

$$\frac{\partial u}{\partial t} + u\frac{\partial u}{\partial x} + v\frac{\partial u}{\partial y} = \nu\frac{\partial^2 u}{\partial y^2} - \frac{\sigma B^2}{\rho}u, \tag{24}$$

$$(\rho c)_f\left(\frac{\partial T}{\partial t} + u\frac{\partial T}{\partial r} + w\frac{\partial T}{\partial z}\right) = k\frac{\partial^2 T}{\partial y^2} - \frac{\partial q_r}{\partial y} + (\rho c)_p\left[D_B\frac{\partial C}{\partial y}\frac{\partial T}{\partial y} + \frac{D_T}{T_\infty}\left(\frac{\partial T}{\partial y}\right)^2\right] + \mu\left(\frac{\partial u}{\partial y}\right)^2, \tag{25}$$

$$\frac{\partial C}{\partial t} + u\frac{\partial C}{\partial x} + v\frac{\partial C}{\partial y} = D_B\frac{\partial^2 C}{\partial y^2} + \frac{D_T}{T_\infty}\frac{\partial^2 T}{\partial y^2}, \tag{26}$$

and new similarity transformations are

$$\psi = \sqrt{\frac{2\nu a}{m+1}}x^{\frac{m+1}{2}}f(\eta,\tau), \quad \eta = y\sqrt{\frac{a(m+1)}{2\nu}}x^{\frac{m-1}{2}},$$
$$\tau = \frac{a(m+1)}{2}x^{m-1}t, \quad \theta(\eta,\tau) = \frac{T - T_\infty}{T_w - T_\infty}, \quad \phi(\eta,\tau) = \frac{C - C_\infty}{C_\infty}. \tag{27}$$

Using Eq. (27) into Eqs. (24)–(26) we obtain,

$$\frac{\partial^3 f}{\partial\eta^3} + f\frac{\partial^2 f}{\partial\eta^2} - \beta\left(\frac{\partial f}{\partial\eta}\right)^2 - M^2\frac{\partial f}{\partial\eta} - \frac{\partial^2 f}{\partial\tau\partial\eta} = 0, \tag{28}$$

$$\left(1 + \frac{4R}{3}\right)\frac{\partial^2\theta}{\partial\eta^2} + Nb\frac{\partial\theta}{\partial\eta}\frac{\partial\phi}{\partial\eta} + Nt\left(\frac{\partial\theta}{\partial\eta}\right)^2 + Pr\left[Ec\left(\frac{\partial^2 f}{\partial\eta^2}\right)^2 + f\frac{\partial\theta}{\partial\eta} - \frac{\partial\theta}{\partial\tau}\right] = 0, \tag{29}$$

$$\frac{\partial^2\phi}{\partial\eta^2} + Scf\frac{\partial\phi}{\partial\eta} + \frac{Nt}{Nb}\frac{\partial^2\theta}{\partial\eta^2} - \frac{\partial\phi}{\partial\tau} = 0, \tag{30}$$

along with boundary conditions

$$f(0,\tau) = s, \quad \frac{\partial f}{\partial\eta}(0,\tau) = \chi + \lambda\frac{\partial^2 f}{\partial\eta^2}(0,\tau),$$
$$\theta(0,\tau) = 1 + \delta\frac{\partial\theta}{\partial\eta}(0,\tau), \quad Nb\frac{\partial\phi}{\partial\eta}(0,\tau) + Nt\frac{\partial\theta}{\partial\eta}(0,\tau) = 0,$$
$$\text{as } \eta \to \infty, \quad \frac{\partial f}{\partial\eta}(\eta,\tau) = 0, \quad \theta(\eta,\tau) = 0, \quad \phi(\eta,\tau) = 0. \tag{31}$$

As suggested by Merkin [44], and Harris et al. [45], the stability of the steady flow solution $f(\eta) = f_0(\eta)$, $\theta(\eta) = \theta_0(\eta)$ and $\phi(\eta) = \phi_0(\eta)$ which satisfies the boundary value problem (14)–(17), can be investigated by considering eigenvalue parameter α with the following relations:

$$f(\eta,\tau) = f_0(\eta) + e^{-\alpha\tau}F(\eta,\tau),$$
$$\theta(\eta,\tau) = \theta_0(\eta) + e^{-\alpha\tau}G(\eta,\tau), \tag{32}$$
$$\phi(\eta,\tau) = \phi_0(\eta) + e^{-\alpha\tau}H(\eta,\tau),$$

where $F(\eta,\tau), G(\eta,\tau)$ and $H(\eta,\tau)$ are small relative to $f_0(\eta), \theta_0(\eta)$ and $\phi_0(\eta)$, respectively.

Using relations (32) into Eqs. (28)–(31) we get the following linear system:

$$\frac{\partial^3 F}{\partial\eta^3} + \frac{\partial^2 f_0}{\partial\eta^2}F + f_0\frac{\partial^2 F}{\partial\eta^2} - 2\beta\frac{\partial f_0}{\partial\eta}\frac{\partial F}{\partial\eta} - M^2\frac{\partial F}{\partial\eta} - \frac{\partial^2 F}{\partial\tau\partial\eta} + \alpha\frac{\partial F}{\partial\eta} = 0, \tag{33}$$

$$\left(1 + \frac{4R}{3}\right)\frac{\partial^2 G}{\partial\eta^2} + Nb\left(\frac{\partial\phi_0}{\partial\eta}\frac{\partial G}{\partial\eta} + \frac{\partial\theta_0}{\partial\eta}\frac{\partial H}{\partial\eta}\right) + 2Nt\frac{\partial\theta_0}{\partial\eta}\frac{\partial G}{\partial\eta} + \frac{\partial\theta_0}{\partial\eta}F + \Pr\left(f_0\frac{\partial G}{\partial\eta} + 2Ec\frac{\partial^2 f_0}{\partial\eta^2}\frac{\partial^2 F}{\partial\eta^2} - \frac{\partial G}{\partial\tau} + \alpha G\right) = 0, \tag{34}$$

$$\frac{\partial^2 H}{\partial\eta^2} + Sc\left(f_0\frac{\partial H}{\partial\eta} + \frac{\partial\phi_0}{\partial\eta}\right) + \frac{Nt}{Nb}\frac{\partial^2 G}{\partial\eta^2} + -\frac{\partial H}{\partial\tau} + \alpha H = 0, \tag{35}$$

$$F(0,\tau) = s, \quad \frac{\partial F}{\partial\eta}(0,\tau) = \lambda\frac{\partial^2 F}{\partial\eta^2}(0,\tau), \quad G(0,\tau) = \delta\frac{\partial G}{\partial\eta}(0,\tau),$$
$$Nb\frac{\partial H}{\partial\eta}(0,\tau) + Nt\frac{\partial G}{\partial\eta}(0,\tau) = 0,$$
$$\text{as } \eta \to \infty, \quad \frac{\partial F}{\partial\eta}(\eta,\tau) = 0, \quad G(\eta,\tau) = 0, \quad H(\eta,\tau) = 0. \tag{36}$$

Now the stability of the solutions $f(\eta) = f_0(\eta), \theta(\eta) = \theta_0(\eta)$ and $\phi(\eta) = \phi_0(\eta)$ of steady problem (14)–(17) can be discussed by putting $\tau = 0$ and then we obtain

$$F_0''' + f_0''F_0 + f_0F'' - 2\beta f_0'F_0' - M^2F_0' + \alpha F_0' = 0, \tag{37}$$

$$\left(1+\frac{4R}{3}\right)G_0''+Nb(\phi_0'G_0'+\theta_0'H_0')+2Nt\theta_0'G_0' + \Pr\left(f_0G_0'+\theta_0'F+2Ecf_0''F_0''+\alpha G_0\right)=0, \quad (38)$$

$$H_0''+Sc\left(\phi_0'F_0+f_0H_0'\right)+\frac{Nt}{Nb}G_0''+\alpha H_0=0, \quad (39)$$

along with boundary conditions

$$F_0(0)=0, \quad F_0'(0)=\lambda F_0''(0), \quad G_0(0)=\delta G_0'(0),$$
$$NbH_0'(0)+NtG_0'(0)=0,$$

$$\text{as } \eta\to\infty, F_0'(\eta)=0, G_0(\eta)=0, H_0(\eta)=0, \quad (40)$$

where $F=F_0(\eta)$, $G=G_0(\eta)$ and $H=H_0(\eta)$ characterize the initial growth and decay of the solution (32). To solve the linear eigenvalue problem (37)–(39) with boundary conditions (40), we relax the condition $F_0'(\eta)\to 0$ as $\eta\to\infty$ and use new boundary condition $F_0''(0)=1$, [45].

4. Numerical solution and validation

The nonlinear ordinary differential Eqs. (14)–(16) along with boundary conditions (17) are solved numerically using shooting technique by converting into initial value problem (IVP). We have placed Eqs. (14)–(16) as first order differential equations by assuming $(f,f',f'',\theta,\theta',\phi,\phi')=(U_1,U_2,U_3,U_4,U_5,U_6,U_7)=U$, as given below:

$$\begin{pmatrix}U_1'\\U_2'\\U_3'\\U_4'\\U_5'\\U_6'\\U_7'\end{pmatrix}=\begin{pmatrix}U_2\\U_3\\-U_1U_3+\beta U_2^2+M^2U_2\\U_5\\-\frac{1}{1+\frac{4R}{3}}\left[\Pr\left(U_1U_5+EcU_3^2\right)+NbU_5U_7+NtU_5^2\right]\\U_7\\-\left(ScU_1U_7+\frac{Nt}{Nb}U_5'\right)\end{pmatrix}, \quad (41)$$

with the initial conditions

$$U^T=\left(s,\chi+\lambda U_3,U_3,1+\delta U_5,U_5,U_6,-\frac{Nt}{Nb}U_5\right)^T. \quad (42)$$

Here it is noticed that without knowing the values of U_3, U_5 and U_6, i.e. $f''(0)$, $\theta'(0)$ and $\phi(0)$, we are not able to solve above system of Eq. (41) with initial conditions (42), which are unknown in this problem; therefore, the most important step of this technique is to pick the suitable values of these unknowns. For this we choose initial values for $f''(0)$, $\theta'(0)$ and $\phi(0)$, such that far field conditions, i.e. $f'(\infty)=0,\theta(\infty)=0,\phi(\infty)=0$, are satisfied with appropriate domain length η_∞ and improve chosen values iteratively by Newton-Raphson method. After getting all the initial conditions, we solve the initial value problem using MATLAB code for RKF45 method. An iterative process is assumed to give a convergent solution when the following condition is satisfied:

$$\sum_i\left|\Omega_i^n-\Omega_i^{n-1}\right|\leqslant 10^{-6}.$$

We have compared the $\{-\theta'(0)\}$ and $\{-\phi'(0)\}$ with earlier published results by [46,2] in Tables 1 and 2 respectively, to validate the accuracy of present numerical results. Skin friction is also compared with exact solution for without slip condition in Table 3. The graphical validation for velocity profile $f'(\eta)$ between exact and numerical solution demonstrated by Fang et al. [29], is shown in Fig. 2. The outstanding agreement is reported for all the results.

5. Results and discussion

The analysis of the present problem has been done numerically. Numerical results of skin friction $f''(0)$, Nusselt Number, temperature $\theta(\eta)$ and nanoparticle concentration $\phi(\eta)$ are presented graphically for different values of governing parameters in Figs. 3–12. We have fixed default values for governing parameters as $R=0.1$, $\beta=1.5$, $M=0.1$, $Ec=0.1$, $s=3.0$, $\Pr=6.8$, $Sc=10$, $Nb=0.5$, $Nt=0.5$, $\lambda=0.1$ and $\delta=0.1$

Table 1 Comparison of results for $-\theta'(0)$ and $-\phi'(0)$ when $M=s=R=Ec=0$, $Pr=10=Sc$, and $\delta=0$ for different values of Nb, Nt and λ for linear stretching sheet $\chi=1$.

Nb	Nt	$\lambda=0$		$\lambda=1$	
		Noghrehabadi et al. [46]	Present results	Noghrehabadi et al. [46]	Present results
$-\theta'(0)$					
0.1	0.1	0.952377	0.952377	0.718928	0.718928
	0.3	0.520079	0.520079	0.392596	0.392596
	0.5	0.321054	0.321054	0.242357	0.242357
0.3	0.1	0.252156	0.252155	0.190347	0.190346
	0.3	0.135514	0.135514	0.102297	0.102296
	0.5	0.083298	0.083298	0.062880	0.062880
$-\phi'(0)$					
0.1	0.1	2.129394	2.129395	1.607430	1.607431
	0.3	2.528638	2.528639	1.908809	1.908810
	0.5	3.035142	3.035144	2.291156	2.291157
0.3	0.1	2.410019	2.410019	1.819268	1.819269
	0.3	2.608819	2.608820	1.969337	1.969338
	0.5	2.751875	2.751877	2.077327	2.077328

Table 2 Comparison of $\{-\theta'(0)\}$ and $\{-\phi'(0)\}$ for different values of Nt and Nb with fixed nanoparticle concentration and no slip condition on the surface, when $Pr=10=Sc$, $Ec=0=M=s=R$ for linear stretching sheet $\chi=1$.

Nt	Nb	$-\theta'(0)$		$-\phi'(0)$	
		Khan and Pop [2]	Present	Khan and Pop [2]	Present
0.1	0.1	0.9524	0.952376	2.1294	2.129388
	0.3	0.2522	0.252155	2.4100	2.410015
	0.5	0.0543	0.054253	2.3836	2.383567
0.3	0.1	0.5201	0.520079	2.5286	2.528625
	0.3	0.1355	0.135514	2.6088	2.608812
	0.5	0.0291	0.029135	2.4984	2.498367
0.5	0.1	0.3211	0.321054	3.0351	3.035120
	0.3	0.0833	0.083298	2.7519	2.751866
	0.5	0.0179	0.017922	2.5731	2.573099

Table 3 Comparison of skin friction at the wall $f''(0)$ with exact solution in case of shrinking sheet $\chi = -1$ for no slip flow ($\lambda = 0, \delta = 0$).

s	M	Exact solution [10]		Present result	
		First	Second	First	Second
3.0	0.1	2.622497	0.377503	2.622498	0.377503
	0.3	2.657584	0.342416	2.657584	0.342416
	0.5	2.724745	0.275255	2.724745	0.275255
4.0	0.1	3.734935	0.265065	3.734935	0.265065
	0.3	3.757840	0.242160	3.757840	0.242160
	0.5	3.802776	0.197224	3.802776	0.197224

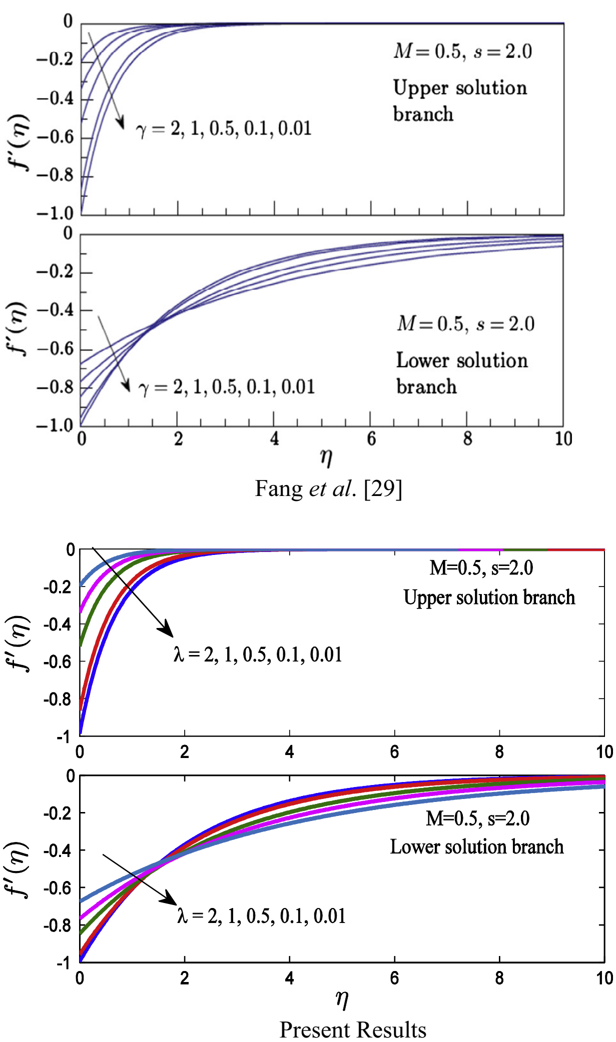

Figure 2 The graphical comparison with exact solution of velocity profile given by Fang et al. [29] at magnetic field $M = 0.5$ and mass transfer parameter $s = 2.0$ for different values of velocity slip parameter λ for shrinking sheet $\chi = -1$.

throughout the computations. First and second solutions are displayed with solid and dotted lines respectively. Since the study considers the dual solutions for the present problem, the physical existence of both first and second solutions is

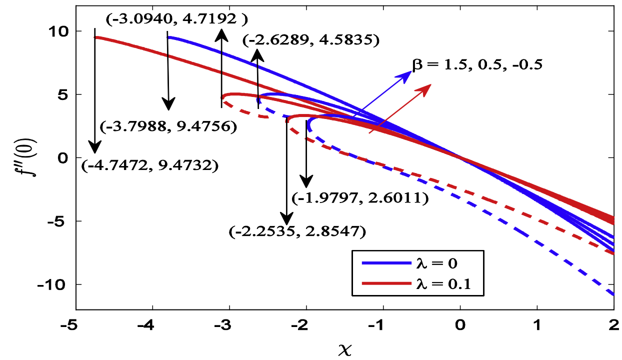

Figure 3 Skin friction $f''(0)$ with stretching parameter χ for different values of power-law parameter β.

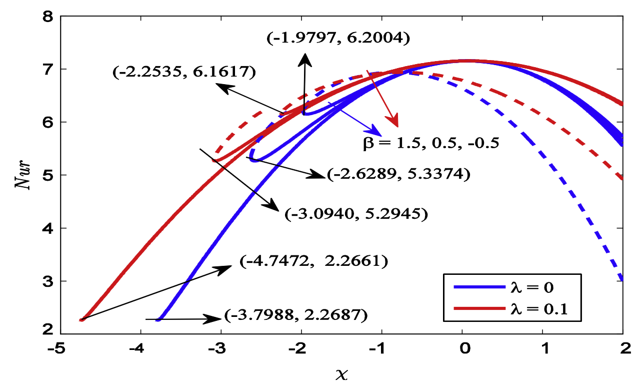

Figure 4 The Nusselt number at the surface with stretching parameter χ for different values of power-law parameter β.

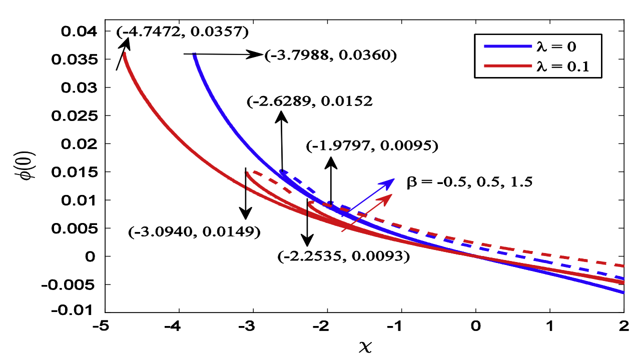

Figure 5 The nanoparticle volume fraction at the surface with stretching parameter χ for different values of power-law parameter β.

investigated by performing stability analysis. We have found the smallest eigenvalues α for some values of involving parameters and results are shown in Table 4. It can be seen that the smallest eigenvalues are positive and negative for the first and second solutions, respectively. The positive eigenvalue corresponds to physically stable solution whereas negative to unstable [44,45]. Hence the first solution is physically stable and second is unstable. Numerical results of $\{-\theta'(0)\}$ have been shown in Table 5 for different values of governing parameters.

Please cite this article in press as: Rana P et al., Radiative nanofluid flow and heat transfer over a non-linear permeable sheet with slip conditions and variable magnetic field: Dual solutions, Ain Shams Eng J (2015), http://dx.doi.org/10.1016/j.asej.2015.08.016

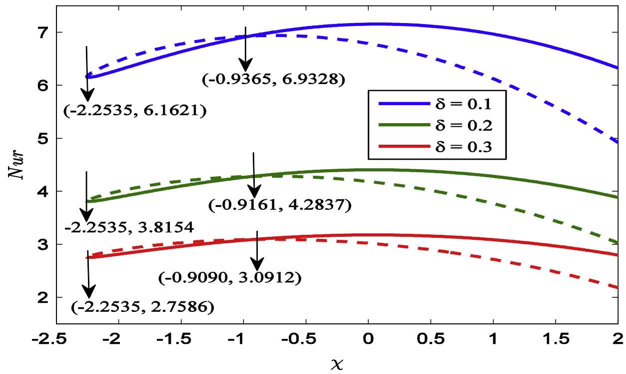

Figure 6 The Nusselt number at surface with stretching parameter χ for different values of thermal slip parameter δ.

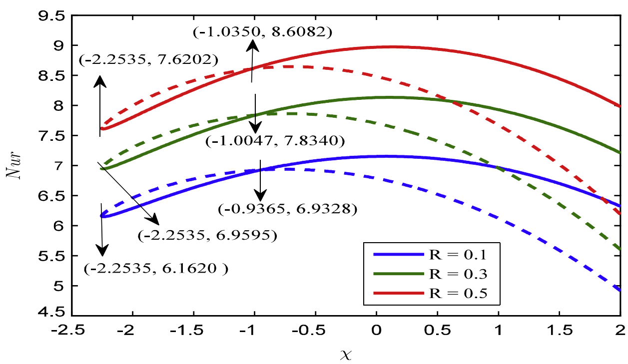

Figure 7 The Nusselt number at surface with stretching parameter χ for different values of thermal radiation parameter R.

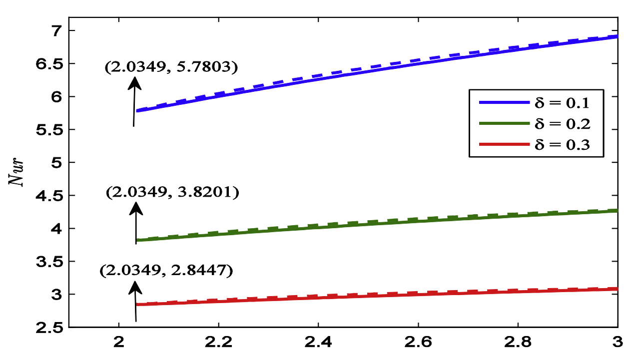

Figure 8 The Nusselt number with mass transfer parameter s for different values of thermal slip parameter δ.

Figs. 3–5 present the influences of power-law parameter β and velocity slip parameter λ, on the skin friction $f''(0)$, Nusselt number and nanoparticle volume fraction $\phi(0)$ for different values of stretching parameter χ. The dual solutions are obtained for $\beta > 0$ while only single solution is obtained when β goes to negative and these solutions are terminated by critical value χ_c. It can also be seen that beyond χ_c ($\chi < \chi_c$), no solution exists and this critical value shifts on left side with β and λ. It is observed that for skin friction, both the solutions are decreasing with an increase in β but opposite behavior is observed for increasing value of λ. The Nusselt number increases with λ and attains maximum value near $\chi = 0$ (static) after that it goes down to the Nusselt number at critical value χ_c. The Nusselt number at the surface enhances as an increase in power-law parameter. Nanoparticle volume fraction increases as power-law parameter increases whereas decreases with increasing value of velocity slip parameter.

The effects of thermal slip parameter δ and thermal radiation R on the Nusselt number are shown in Figs. 6 and 7. It can be seen that the solution does not exist beyond the critical value $\chi_c = -2.2535$ and the first and second both the solutions are decreasing with increasing values of thermal slip parameter δ and increasing with thermal radiation R. Here it can also be noted that for particular value of χ near to -1 the Nusselt number has unique value and first and second solutions have opposite behavior on left and right of this particular value. For δ = 0.1, 0.2 and 0.3, the particular value χ_{pv} is -0.9365, -0.9161 and -0.9090 respectively. Similarly, for R = 0.1, 0.3 and 0.5, χ_{pv} is -0.9365, -1.0047 and -1.0350 respectively.

Further, the effect of mass transfer parameter s on the Nusselt number for different values of thermal slip parameter δ is investigated (see Fig. 8) and observed that the Nusselt number is decreasing with δ and s. The critical value s_c remains unchanged with δ such that no solution exists for $s < s_c$ and first solution is found lower than second solution.

The variation of the Nusselt number with R for various values of Nt and s is shown in Fig. 9 in the presence and absence of thermal slip parameter δ. The Dual solutions are captured such that first solution is always higher than second solution. As Nusselt number is ratio of convective and conductive heat transfer so for large Nusselt number, heat convection rises. The Nusselt number is decreasing with Nt and δ but increasing with thermal radiation R and mass transfer parameter s.

Fig. 10 gives the effect of viscous dissipation parameter Ec (Eckert number, which controls the fluid flow), on the local Nusselt number for several values of Prandtl number Pr and Schmidt number Sc. It is observed that for both solutions, the local Nusselt number is decreasing, with Ec and Sc but increasing with Pr. Here it is interesting to see that the first solution is higher than second solution in the absence of viscous dissipation (Ec = 0) while opposite trend is observed in the presence of viscous dissipation (Ec = 0.1, 0.2).

The influence of thermal radiation on temperature $\theta(\eta)$ and nanoparticle volume fraction $\phi(\eta)$ is displayed in Fig. 11. As the value of thermal radiation R increases, temperature and nanoparticle volume fraction increase. Moreover, temperature gradient and thermal boundary layer thickness decrease.

Further, the effect of nanofluid parameters (Brownian motion parameter Nb and thermophoresis parameter Nt) on nanoparticle volume fraction has been investigated. The gradient of nanoparticle concentration at the surface is controlled passively by the product of temperature gradient and ($-Nt/Nb$) therefore nanoparticle concentration gradient increases with Nt and decreases with Nb for fixed temperature gradient. From Fig. 12 it can be observed that nanoparticle volume fraction is increasing with Nt, which is due to the fact that thermophoretic force takes away the fluid from the surface quickly, which leads to an increase in the concentration boundary layer thickness. On the other hand nanoparticle volume fraction decreases with an increasing value of Nb and concentration boundary layer thickness reduces.

Please cite this article in press as: Rana P et al., Radiative nanofluid flow and heat transfer over a non-linear permeable sheet with slip conditions and variable magnetic field: Dual solutions, Ain Shams Eng J (2015), http://dx.doi.org/10.1016/j.asej.2015.08.016

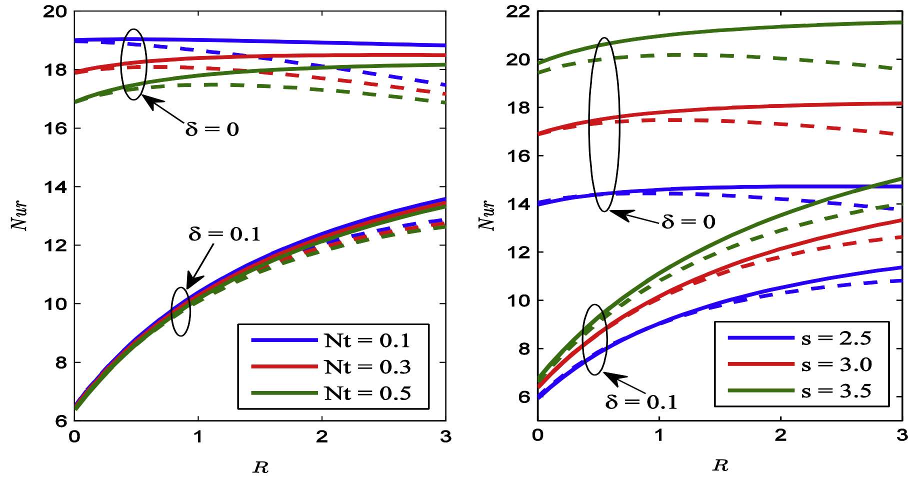

Figure 9 The effect of thermophoresis parameter Nt and mass transfer parameter s on the Nusselt number with thermal radiation R for different values of thermal slip parameter δ.

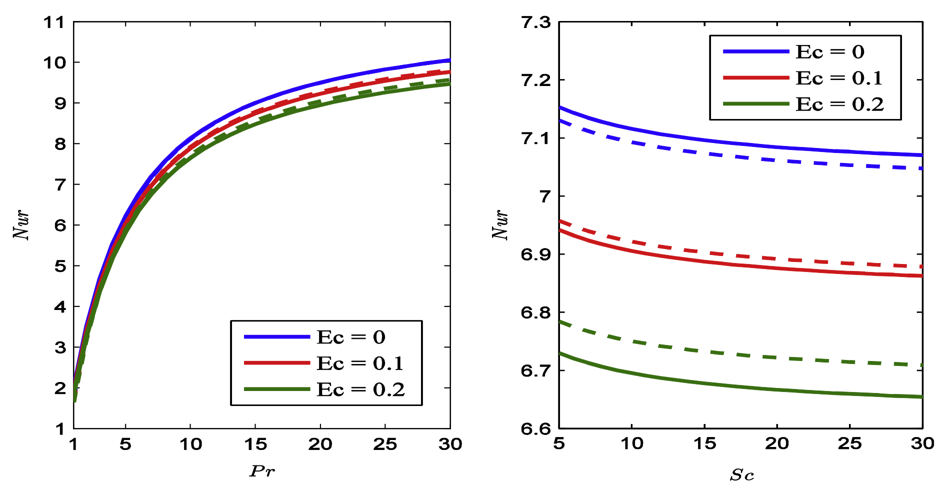

Figure 10 The influence of Eckert number Ec on Nusselt number for different values of Prandtl number Pr and Schmidt number Sc.

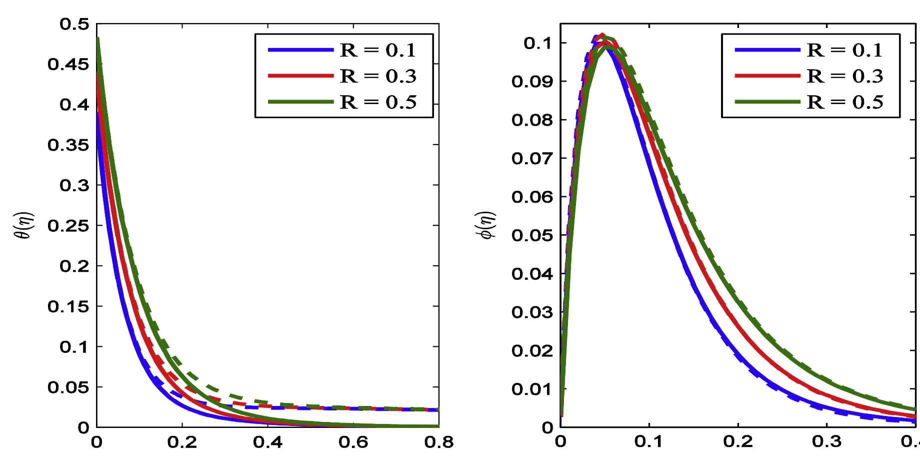

Figure 11 The effect of thermal radiation R on temperature $\theta(\eta)$ and nanoparticle volume fraction $\phi(\eta)$.

Please cite this article in press as: Rana P et al., Radiative nanofluid flow and heat transfer over a non-linear permeable sheet with slip conditions and variable magnetic field: Dual solutions, Ain Shams Eng J (2015), http://dx.doi.org/10.1016/j.asej.2015.08.016

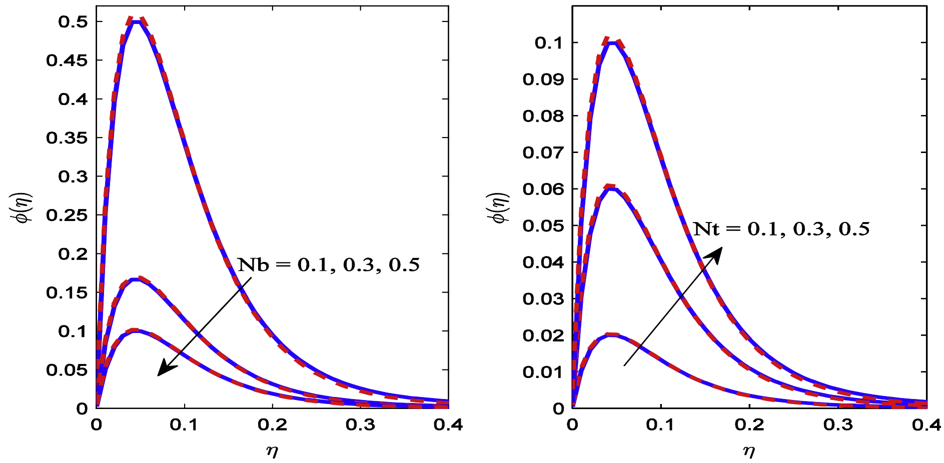

Figure 12 The effect of nanofluid parameters (Nb and Nt) on nanoparticle concentration $\phi(\eta)$.

Table 4 The smallest eigenvalues α for first and second solutions with different values of s, χ, λ and β, while other parameters are fixed.

s	$\lambda = 0$		s	$\lambda = 0.1$	
	First solution	Second solution		First solution	Second solution
2.2	0.4131	−0.3887	2.05	0.1808	−0.1766
2.14	0.1635	−0.1602	2.04	0.1013	−0.1001
2.13	0.0630	−0.0629	2.038	0.0759	−0.0757
χ	$\beta = 0.5$		χ	$\beta = 1.5$	
−3.07	0.2023	−0.1853	−2.15	0.6793	−0.6510
−3.08	0.1522	−0.1430	−2.20	0.4890	−0.4758
−3.085	0.1203	−0.1148	−2.22	−0.3783	−0.3780

Table 5 Numerical values of first and second solution (given in brackets) of $\{-\theta'(0)\}$ for different values of M, λ, δ, R and Nt for power-law shrinking sheet $\chi = -1$ when other parameters are fixed.

M	R	(λ, δ)	Nt		
			0.1	0.3	0.5
0.2	0.1	(0.1, 0.1)	6.189207	6.141767	6.092976
			(6.195208)	(6.149257)	(6.102025)
		(0.1, 0.2)	3.782973	3.771844	3.760436
			(3.779945)	(3.780431)	(3.769725)
		(0.2, 0.1)	6.253965	6.206668	6.158027
			(6.188265)	(6.142379)	(6.095217)
0.2	0.1	(0.1, 0.1)	6.189207	6.141767	6.092976
			(6.195208)	(6.149257)	(6.102025)
	0.3		5.696319	5.647115	5.596775
			(5.691942)	(5.644108)	(5.595198)
	0.5		5.274784	5.225663	5.175644
			(5.259762)	(5.211896)	(5.163182)
0	0.1	(0.1, 0.1)	6.189786	6.142357	6.093578
			(6.202492)	(6.156475)	(6.109174)
0.2			6.189207	6.141767	6.092976
			(6.195208)	(6.149257)	(6.102025)
0.5			6.186358	6.138862	6.090012
			(6.146766)	(6.101274)	(6.054522)

6. Conclusion

The numerical investigation has been carried out in this study to analyze the influence of governing over a stretching/shrinking sheet under the slip flow of nanofluid. The governing partial differential equations are formulated into nonlinear ordinary differential equations of non-dimensional parameters by using similarity variables and being solved numerically by RKF45 method with shooting technique. We have acquired interesting observations graphically for these pertinent parameters which are summarized below:

- The critical values (χ_c and s_c) are found for the existence of both first and second solutions.
- At the surface, Skin friction decreases whereas Nusselt number and nanoparticle volume fraction increase with increasing value of power-law parameter. Skin friction increases as velocity slip parameter increases.
- The Nusselt number decreases with an increase of thermophoresis parameter, thermal slip parameter, viscous dissipation and Schmidt number but increases with thermal radiation, mass transfer parameter and Prandtl number.
- It is observed that temperature and nanoparticle volume fraction enhance with thermal radiation. Moreover, nanoparticle volume fraction increases with thermophoresis parameter and decreases with Brownian motion parameter.

References

[1] Crane LJ. Flow past a stretching plate. Appl Math Phys 1970;21:645–7.
[2] Khan WA, Pop I. Boundary-layer flow of a nanofluid past a stretching sheet. Int J Heat Mass Transf 2010;53:2477–83.
[3] Cortell R. Viscous flow and heat transfer over a nonlinearly stretching sheet. Appl Math Comput 2007;184:864–73.
[4] Rana P, Bhargava R. Flow and heat transfer over a nonlinearly stretching sheet: a numerical study. Commun Nonlin Sci Numer Simul 2012;17:212–26.
[5] Nadeem S, Lee C. Boundary layer flow of nanofluid over an exponentially stretching surface. Nanosc Res Lett 2012;7.
[6] Choi US, Eastman JA. Enhancing thermal conductivity of fluids with nanoparticles. In: ASME international mechanical engineering congress and exposition. San Francisco; 1995.
[7] Buongiorno J. Convective transport in nanofluids. ASME J Heat Transf 2006;128:240–50.
[8] Kuznetsov AV, Nield DA. Natural convection boundary-layer of a nanofluid past a vertical plate: a revised model. Int J Therm Sci 2014;77:126–9.
[9] Ganesan P, Palani G. Finite difference analysis of unsteady natural convection MHD flow past an inclined plate with variable surface heat and mass flux. Int J Heat Mass Transf 2004;47:4449–57.
[10] Fang T, Zhang J. Closed-form exact solution of MHD viscous flow over a shrinking sheet. Commun Nonlin Sci Numer Simul 2009;14:2853–7.
[11] Hamad MAA. Analytical solution of natural convection flow of a nanofluid over a linearly stretching sheet in the presence of magnetic field. Int Commun Heat Mass Transf 2011;38:487–92.
[12] Rana P, Bhargava R, Beg OA. Finite element simulation of unsteady magneto-hydrodynamic transport phenomena on a stretching sheet in a rotating nanofluid. J Nanoeng Nanosyst 2011;227:77–99.
[13] Sheikholeslami M, Hatami M, Ganji DD. Nanofluid flow and heat transfer in a rotating system in the presence of a magnetic field. J Molecul Liq 2014;190:112–20.
[14] Uddin MdJ, Khan WA, Ismail MdAI. Scaling group transformation for MHD boundary layer slip flow of a nanofluid over a convectively heated stretching sheet with heat generation. Math Prob Eng 2012;2012.
[15] Shehzad SA, Abbasi FM, Hayat T, Alsaadi F. MHD mixed convective peristaltic motion of nanofluid with Joule heating and thermophoresis effects. Plos One 2014;9.
[16] Uddin MdJ, Beg OA, Aziz A, Ismail AI. Group analysis of free convection flow of a magnetic nanofluid with chemical reaction. Math Prob Eng 2015;2015.
[17] Abbasi FM, Shehzad SA, Hayat T, Alsaedi A, Mustafa AO. Influence of heat and mass flux conditions in hydromagnetic flow of Jeffrey nanofluid. AIP Adv 2015;5:037111.
[18] Mabood F, Khan WA, Ismail AIM. MHD boundary layer flow and heat transfer of nanofluids over a nonlinear stretching sheet: a numerical study. J Magnet Magnet Mater 2015;374:569–76.
[19] Seddeek MA. Effects of radiation and variable viscosity on a MHD free convection flow past a semi-infinite flat plate with an aligned magnetic field in the case of unsteady flow. Int J Heat Mass Transf 2001;45:931–5.
[20] Cortell R. Effect of viscous dissipation and radiation on the thermal boundary layer over a non-linearly stretching sheet. Phys Lett A 2008;372:631–6.
[21] Hady FM, Ibrahim FS, Abdel-Gaied SM, Eid MR. Radiation effect on viscous flow of a nanofluid and heat transfer over a nonlinearly stretching sheet. Nanosc Res Lett 2012;7.
[22] Motsumi TG, Makinde OD. Effects of thermal radiation and viscous dissipation on boundary layer flow of nanofluids over a permeable moving flat plate. Phys Script 2012;86.
[23] Pal D, Mandal G, Vajravelu K. MHD convection–dissipation heat transfer over a non-linear stretching and shrinking sheets in nanofluids with thermal radiation. Int J Heat Mass Transf 2013;65:481–90.
[24] Nandy SK, Pop I. Effects of magnetic field and thermal radiation on stagnation flow and heat transfer of nanofluid over a shrinking surface. Int Commun Heat Mass Transf 2014;53:50–5.
[25] Sheikholeslami M, Ganji DD, Javed MY, Ellahi R. Effect of thermal radiation on magnetohydrodynamics nanofluid flow and heat transfer by means of two phase model. J Magnet Magnet Mater 2014.
[26] Rashidi MM, Ganesh NV, Hakeem AKA, Ganga B. Buoyancy effect on MHD flow of nanofluid over a stretching sheet in the presence of thermal radiation. J Molec Liq 2014;198:234–8.
[27] Navier CLMH. Memoire sur les lois du mouvement des fluides. Mem Acad R Sci Inst France 1823;6:389–440.
[28] Wang CY. Flow due to a stretching boundary with partial slip-an exact solution of the Navier–Stokes equation. Chem Eng Sci 2002;57:3745–7.
[29] Fang T, Zhang J, Yao S. Slip magnetohydrodynamic viscous flow over a permeable shrinking sheet. Chin Phys Lett 2010;27.
[30] Das K. Slip flow and convective heat transfer of nanofluids over a permeable stretching surface. Comp Fluids 2012;64:34–42.
[31] Das K. Nanofluid flow over a nonlinear permeable stretching sheet with partial slip. J Egypt Math Soc 2014.
[32] Ibrahim W, Shankar B. MHD boundary layer flow and heat transfer of a nanofluid past a permeable stretching sheet with velocity, thermal and solutal slip boundary conditions. Comp Fluids 2013;75:1–10.
[33] Uddin MJ, Beg OA, Amin N. Hydromagnetic transport phenomena from a stretching or shrinking nonlinear nanomaterial sheet with Navier slip and convective heating: a model for bio–nano-materials processing. J Magnet Magnet Mater 2014;368:252–61.
[34] Turkyilmazoglu M. Dual and triple solutions for MHD slip flow of non-Newtonian fluid over a shrinking surface. Comp Fluids 2012;70:53–8.
[35] Kameswaran PK, Sibanda P, RamReddy C, Murthy PVSN. Dual solution of stagnation-point flow of a nanofluid over a stretching surface. Bound Value Prob 2013;2013(1-12):188.

Please cite this article in press as: Rana P et al., Radiative nanofluid flow and heat transfer over a non-linear permeable sheet with slip conditions and variable magnetic field: Dual solutions, Ain Shams Eng J (2015), http://dx.doi.org/10.1016/j.asej.2015.08.016

[36] Subhashini SV, Sumathi R. Dual solution of a mixed convection flow of nanofluids over a moving vertical plate. Int J Heat Mass Transf 2014;71:117–24.
[37] Subhashini SV, Sumathi R, Momoniat E. Dual solutions of a mixed convection flow near the stagnation point region over an exponentially stretching/shrinking sheet in nanofluids. Meccanica 2014;49:2467–78.
[38] Mansur S, Ishak A, Pop I. Flow and heat transfer of nanofluid past stretching/shrinking sheet with partial slip boundary conditions. Appl Math Mech 2014;35:1401–10.
[39] Na TY. Computational method in engineering boundary value problems. New York: Academic Press; 1979.
[40] Shehzad SA, Hussain T, Hayat T, Ramzan M, Alsaedi A. Boundary layer flow of third grade nanofluid with Newtonian heating and viscous dissipation. Central South Univ 2015;22:360–7.
[41] Javed T, Abbas Z, Sajid M, Ali N. Heat transfer analysis for a hydromagnetic viscous fluid over a non-linear shrinking sheet. Int J Heat Mass Transf 2011;54:2034–42.
[42] Hayat T, Hussain T, Shehzad SA, Alsaedi A. Flow of Oldroyd-B fluid with nanoparticles and thermal radiation. Appl Math Mech 2015;36:69–80.
[43] Uddin MdJ, Beg OA, Ismail AI. Radiative convective nanofluid flow past a stretching/shrinking sheet with slip effects. J Thermophys Heat Transf 2015;29:513–23.
[44] Merkin JH. On dual solution occurring in mixed convection in a porous medium. J Eng Math 1985;20:171–9.
[45] Harris SD, Ingham DB, Pop I. Mixed convection boundary layer flow near the stagnation point on a vertical surface in a porous medium: Brinkman model with slip. Transp Porous Media 2009;77:267–85.
[46] Noghrehabadi A, Pourrajab R, Ghalambaz M. Effect of partial slip boundary condition on the flow and heat transfer of nanofluids past stretching sheet prescribed constant wall temperature. Int J Therm Sci 2012;54:253–61.

Dr. Puneet Rana is presently working as a Assistant Professor, Department of Mathematics, Jaypee Institute of Information Technology, Noida, India. He has done his BSc. with silver medal, in S.C.D. Govt College, Ludhiana, Punjab, India, in 2006 and MSc (H.S.) in Department of Mathematics from Panjab University, Chandigarh, Punjab, India, in 2008. He has won National Merit Scholarship in his Graduation. He obtained his Doctorate from Indian Institute of Technology Roorkee, Roorkee, India, in 2013. He has number of publications in various International Journal and Conferences. His research interests include Micropolar fluids, Nanofluids, Stability analysis, Heat transfer and Finite Element method.

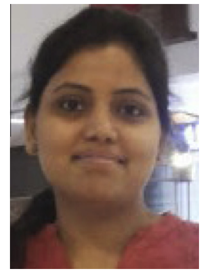

Ruchika Dhanai, born on 27-10-1988 in Dehradun, Uttarakhand, India, is a Research Scholar of Department of Mathematics, Jaypee Institute of Information Technology Noida, India. She did her BSc in D.B.S. (P.G) College Dehradun, Uttarakhand, India, in 2008 and MSc in D.A.V. (P.G) College Dehradun, Uttarakhand, India, in 2010. She is pursuing her PhD under the supervision of Dr. Lokendra Kumar and Dr. Puneet Rana, since 2013. She has cleared Uttarakhand state eligibility test (U-SET) in 2012.

Dr. Lokendra Kumar received PhD in 2004 from IIT Roorkee. He is working as Assistant professor (senior grade) in JIIT and having experience of ten years in teaching and research. He has qualified GATE in 2001 and awarded with CSIR fellowship in 2000. He has published so many research papers in international and national journals. His research interests include Computational Fluid Dynamics, Numerical Methods, FEM and Mesh Free Methods.

Please cite this article in press as: Rana P et al., Radiative nanofluid flow and heat transfer over a non-linear permeable sheet with slip conditions and variable magnetic field: Dual solutions, Ain Shams Eng J (2015), http://dx.doi.org/10.1016/j.asej.2015.08.016